# Simultaneous H/D and $^{13}$C/$^{12}$C anomalous kinetic isotope effects during the sonolysis of water in the presence of carbon monoxide

Sergey I. Nikitenko, Tony Chave, Matthieu Virot, Rachel Pflieger

## HAL Id: cea-03602469
## https://hal-cea.archives-ouvertes.fr/cea-03602469

Submitted on 10 Oct 2022

# Simultaneous H/D and $^{13}$C/$^{12}$C Anomalous Kinetic Isotope Effects during the Sonolysis of Water in the Presence of Carbon Monoxide

Sergey I. Nikitenko,* Tony Chave, Matthieu Virot, and Rachel Pflieger

ICSM, Univ Montpellier, UMR 5257, CEA, CNRS, ENSCM, Marcoule, France

**ABSTRACT:** Splitting of water molecule driven by ultrasound plays a central role in sonochemistry. While studies of sonoluminescence revealed the formation of a plasma inside the cavitation bubble, much less is known about the contribution of plasma chemical processes to the sonochemical mechanisms. Herein, we report for the first time sonochemical processes in water saturated with pure CO. The presence of CO causes a strong increase of the H/D kinetic isotope effect (KIE) up to $\alpha_H$=14.6±1.8 in 10% $H_2O$/$D_2O$ mixture under 20 kHz ultrasound. The anomalous H/D KIE is attributed to electron quantum tunneling in the plasma produced by cavitation. In addition, $CO_2$ formed simultaneously with hydrogen during the sonochemical process is enriched with $^{13}$C isotope, which indicates V-V pumping mechanism typical for non-equilibrium plasma. Both observed KIE unambiguously point out the contribution of quantum effects in sonochemical mechanisms.

**TOC Graphic**
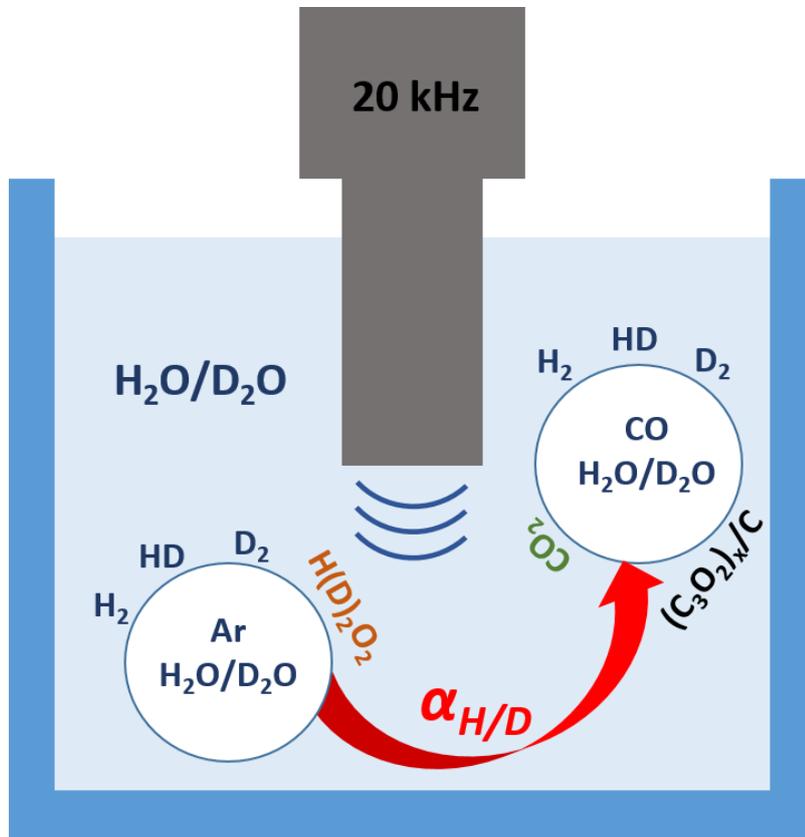
Sonochemistry has a long history, dating back to the works of Richards and Loomis[1] and Schmitt et al.[2] However, the mechanisms of sonochemical reactions are far from trivial and far from being understood. The mainstream concept of the chemical processes driven by power ultrasound is based on the idea of a quasi-adiabatic heating of the gas/vapor mixture inside the inertial cavitation bubbles (hot spot). In terms of hot spot approach, the cavitation bubble has a transient equivalent temperature of roughly 5000 K and a pressure around 1000 bar at the last stage of bubble collapse.[3] The strong local heating is acknowledged to lead to homolytic splitting of molecular bonds, yielding highly reactive radicals. Another mechanism may however also contribute to radical production due to the formation of a non-equilibrium plasma inside the bubble, as revealed by recent spectroscopic studies of sonoluminescence.[4-6] Such a plasma is characterized by the absence of thermal equilibrium: $T_e > T_v > T_r \approx T_g$, where $T_e$ is the electron temperature associated with the ionization degree of the nonequilibrium plasma, $T_v$ is the vibrational temperature, which characterizes the level of excitation of molecular vibrations, and $T_r$ is the rotational temperature often taken as close to gas temperature ($T_g$).[7] Therefore, the intrabubble conditions cannot be described by a single gas temperature. In addition, plasma formation implies a strong contribution of vibrationally-excited and ionized species to the overall mechanism of sonochemical reactions. The formation of ionized species has been observed during single bubble collapse in $H_2SO_4$ using sonoluminescence spectroscopy.[8,9] More recently, it was reported that solvated electrons escaped from a single collapsing bubble enabled to initiate sonochemiluminescence of $Ce^{3+}$ and $Tb^{3+}$ ions in aqueous solutions.[10,11] However, observations of specific plasma chemical effects in sonochemistry are still scarce.

It is known that chemical reactions in plasmas far from equilibrium are often accompanied by unusual kinetic isotope effects (KIE).[7] Recently, a reverse $^{13}C/^{12}C$ KIE was observed in the reaction of ultrasonically driven disproportionation of carbon monoxide in water.[12] The solid carbonaceous product formed during this process in the presence of Ar/CO gas mixture was found to be slightly enriched with the heavier $^{13}C$ isotope, which is not consistent with thermal KIE. In terms of "classical" transition state theory of KIE, light isotopes would react faster because of their higher "zero vibration level".[13] On the other hand, in a non-equilibrium plasma CO disproportionation occurs through an anharmonic vibration-to-vibration (V-V) pumping mechanism, called Treanor effect, leading to reverse KIE due to the higher $T_v$ of the vibrationally excited species of heavy isotopes.[7] It is important to emphasize that V-V pumping mechanism does not happen under thermal equilibrium. Therefore, the inverse $^{13}C/^{12}C$ KIE clearly indicates the absence of equilibrium inside the cavitation bubble. In addition, a large H/D KIE has been reported for sonochemical splitting of water molecule in the presence of Ar and Xe.[14] Similar to the KIE observed with CO molecules, the anomalous sonochemical H/D KIE cannot be understood in terms of water molecule thermal splitting. It was hypothesized that the sonochemical H/D KIE deals with quantum electron tunneling like what was observed for water radiolysis.[14] Despite all efforts, the contribution of quantum effects to sonochemistry requires further experimental evidence.

To improve the understanding of the mechanisms engendering isotopic selectivity in sonochemistry, we studied simultaneously H/D and $^{13}C/^{12}C$ KIE during the sonolysis of $D_2O/H_2O$ mixtures saturated with pure CO or 10vol.%CO/Ar gas mixture. In comparison to pure Ar gas, use of Ar/CO gas mixture induces a dramatic decline in the rate of hydrogen peroxide formation. In pure CO, the formation of $H_2O_2$ completely vanishes whatever the composition of the $H_2O/D_2O$ mixture (Figure 1a). By contrast, the formation rate of hydrogen,

$W(\Sigma H_2)$, where $\Sigma H_2 = H_2 + HD + D_2$, strongly increases in the presence of CO reaching a maximum for Ar/CO mixture (Figure 1b). Both phenomena have been attributed to the scavenging of $OH^\bullet$ radicals with CO :[12]

$H_2O$ $—)))\rightarrow$ $H$ $+$ $OH^\bullet$
(1)

$OH^\bullet+$ $CO$ $\rightarrow$ $H$ $+$ $CO_2$
(2)

$2H \rightarrow H_2$ (3)

where ))) symbolizes a process induced by cavitation event. To the best of our knowledge, this is the first observation of the sonochemical splitting of water molecule in the presence of pure CO. It is worth noting that the specific heat ratio, $\gamma = C_p/C_v$, is lower for CO ($\gamma = 1.40$) than for Ar ($\gamma = 1.667$).[15] In addition, the thermal conductivity of CO (25 mW·m$^{-1}$·K$^{-1}$ at 300 K) is larger than that of Ar (17.9 mW·m$^{-1}$·K$^{-1}$ at 300 K).[15] Therefore, no significant $H_2O$ splitting would be expected with CO as a saturating gas according to the quasi-adiabatic heating model of cavitation. Instead, the observed sonochemical activity with CO can be understood in terms of a plasma chemical approach. In fact, the ionization potential of CO (14.01 eV) is less than of Ar (15.76 eV) and very close to that of Kr (13.99 eV), which would favor plasma formation. On the other hand, the vibrational excitation of CO would require 5.5 eV·mol$^{-1}$ according to published data[7] leading to some dissipation of excitation energy during bubble collapse. Therefore, the overall sonochemical activity with CO should be lower when compared to Ar/CO mixture, which is in agreement with the experimental results (Figure 1b). It should also be noted that $H_2O_2$ and $H_2$ formation rates in Ar and Ar/CO are independent from $H_2O/D_2O$ ratio indicating the similarity of the intrabubble conditions in $H_2O$ and $D_2O$.
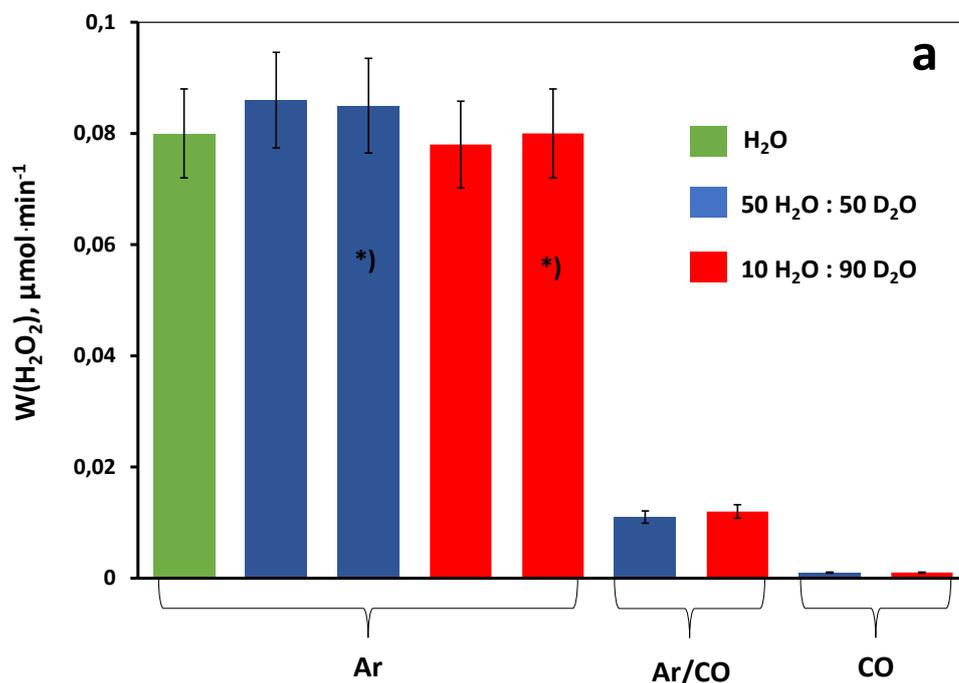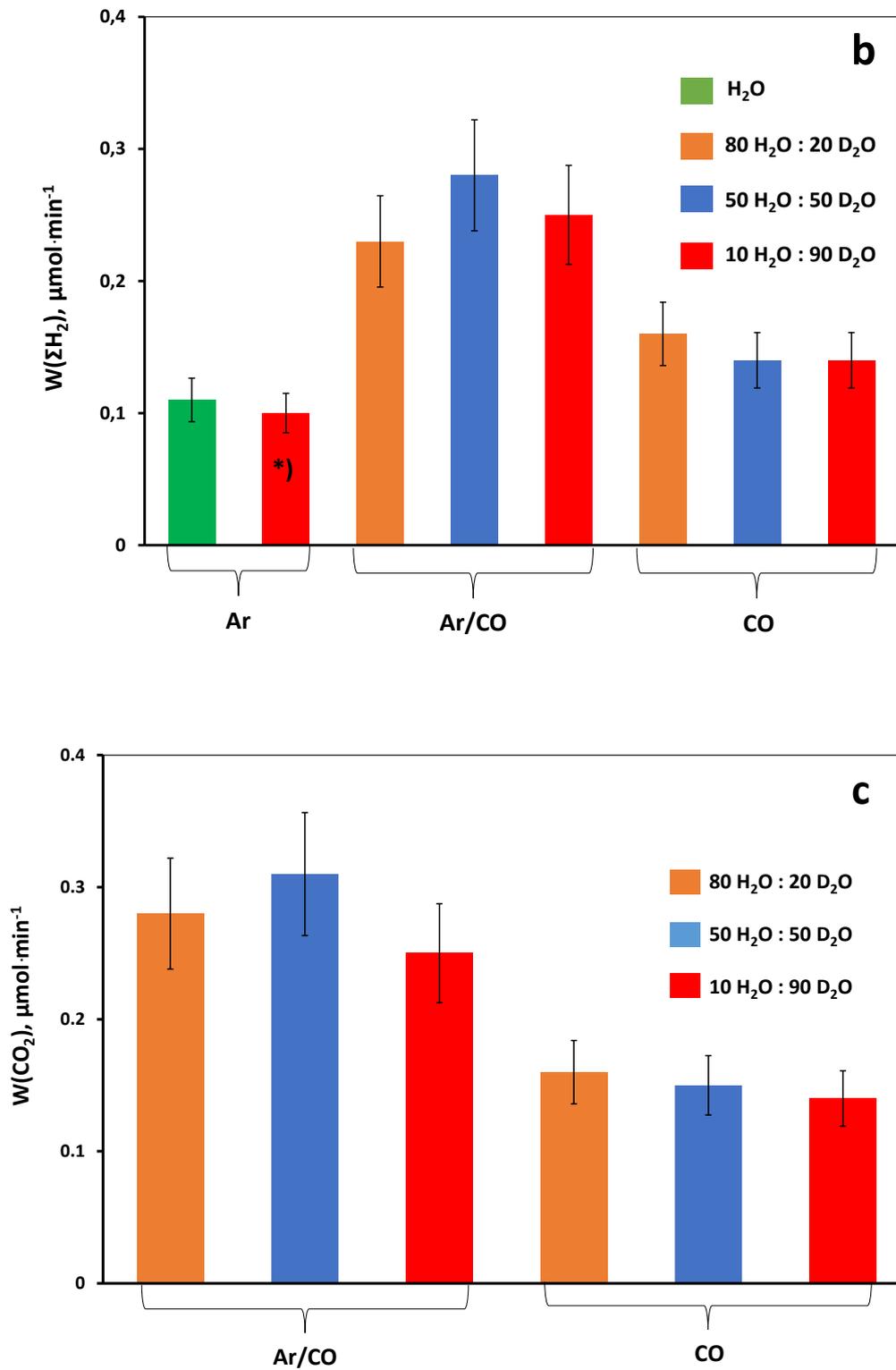
**Figure 1.** Rate of $H_2O_2$ (**a**), $\Sigma H_2$ (**b**), and $CO_2$ (**c**) formation during the ultrasonic treatment of $H_2O/D_2O$ mixtures ($f$ = 20 kHz, $P_{ac}$ = 19±1 W) in the presence of Ar, Ar/10% CO, and CO

saturating gases ($T$ = 20±1°C). In each experiment, the ultrasonic treatment was performed at least 3 h. Then the reaction rate was calculated from zero-order kinetic plots. *⁾ Data from our previous study.[14]


In agreement with reaction **2**, the sonochemical process is accompanied by $CO_2$ release. It is worth noting that neither methane nor other hydrocarbons have been observed under the experimental conditions used in our study. Similarly to $\Sigma H_2$, the kinetics of $CO_2$ formation is not significantly influenced by the isotopic composition of water (Figure 1c). On the other hand, Figure 1c points out a higher reaction rate in the presence of Ar/CO gas mixture compared to pure CO as in the case of hydrogen formation. In addition, TOC analysis shows the presence of ca. 5 and 4 ppm of organic carbon in sonicated solutions with CO and Ar/CO, respectively, implying that CO is not only involved in the reaction with OH$^\bullet$ radical, but also in other processes leading to some organic compounds. The results of ion-chromatography analysis summarized in Table 1 reveals the presence of formic acid as the major product with some amounts of oxalic and acetic acids. Formic acid is most likely formed by direct hydration of CO within the cavitation bubble:
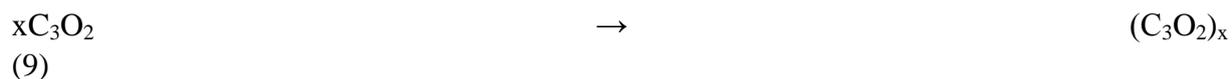
$$CO + H_2O \text{ —)))} \rightarrow HCOOH \tag{4}$$

In a non-equilibrium plasma, reaction **4** is triggered by vibrational excitation of CO ($0 \rightarrow v' = 1, 2\ldots 10$) after 1-3 eV electron impact.[7,16] On the other hand, the thermally activated reaction between CO and $H_2O$, known as water gas-shift process (WGSP), yields $CO_2$ and $H_2$ rather than HCOOH.[17] Oxalic and acetic acids can be formed in sonochemical processes as secondary products of formic acid oxidation by OH$^\bullet$ radicals.[18,19] This assumption is confirmed by the data gathered in Table 1, which demonstrate that the presence of Ar/CO causes a decrease in HCOOH concentration but a larger concentration of $H_2C_2O_4$ when compared to neat CO. As shown in Figure 1a, OH$^\bullet$ radicals are less effectively scavenged in Ar/CO than in CO providing better HCOOH oxidation.

**Table 1**. Ion-chromatography analysis of organic species formed during the ultrasonic treatment of $10H_2O/90D_2O$ mol % mixture in the presence of Ar/10 mol % CO and CO gases. $f$ = 20 kHz, $P$ = 19±1 W, T = 20 °C, time of ultrasonic treatment − 4 h. The details of ion-chromatography analysis are shown in Figure S2.

| Carrier gas | HCOOH ppm | $H_2C_2O_4$ ppm | $CH_3COOH$ ppm |
|---|---|---|---|
| CO | 5.2±0.3 | 0.45±0.02 | 0.6±0.2 |
| Ar/CO | 2.6±0.3 | 1.1±0.1 | 0.5±0.1 |

The ultrasonic treatment of $H_2O/D_2O$ mixtures also causes the formation of a black solid residue. HRTEM (Figure 2a) and STEM/EDX (Figure S3) analyses revealed that this residue is composed of some plate-like carbonaceous particles and submicronic titanium particles with an irregular shape. The latter originate from the cavitation erosion of the ultrasonic horn. The FTIR spectrum of the black solid (Figure 2b) exhibits two broad bands centered at ca. 2350 and 2100 cm$^{-1}$ attributed to $CO_2$ trapped in the solid matrix and C=O bond vibration in ketene group C=C=O respectively.[20] It is interesting to emphasize that

ketene is a fingerprint of polymerized carbon suboxide, $(C_3O_2)_x$, whose formation was reported in non-equilibrium plasmas by a vibrational excitation mechanism:[7]

$$CO + e^- \rightarrow CO* \tag{5}$$

$$CO* + CO* \rightarrow C + CO_2 \tag{6}$$

$$C + CO \rightarrow C_2O \tag{7}$$

$$C_2O + CO \rightarrow C_3O_2 \tag{8}$$

$$xC_3O_2 \rightarrow (C_3O_2)_x \tag{9}$$

On the other hand, the Raman spectrum acquired on the black residue (Figure 2c) shows D (ca. 1350 cm$^{-1}$) and G (ca. 1590 cm$^{-1}$) bands as well as their overtones at 2500-3200 cm$^{-1}$ which are representative of disordered graphitic carbon.[21,22] It is worth noting that $(C_3O_2)_x$ polymer is not stable even at mild temperatures eliminating $CO_2$ and yielding carbon-rich species.[23,24] Therefore, one can conclude that the composition of carbonaceous products agrees well with a plasma-like mechanism of sonochemical process. It also cannot be totally excluded that organic acids observed in solution are formed as a result of $(C_3O_2)_x$ degradation.
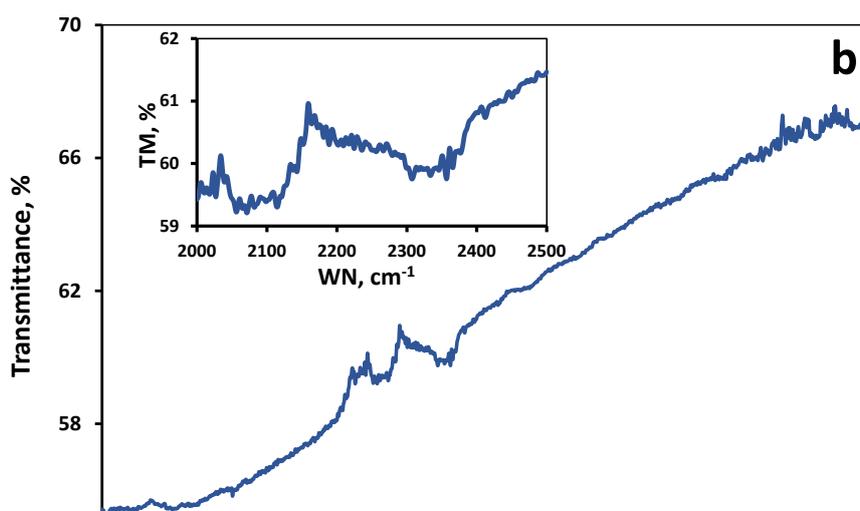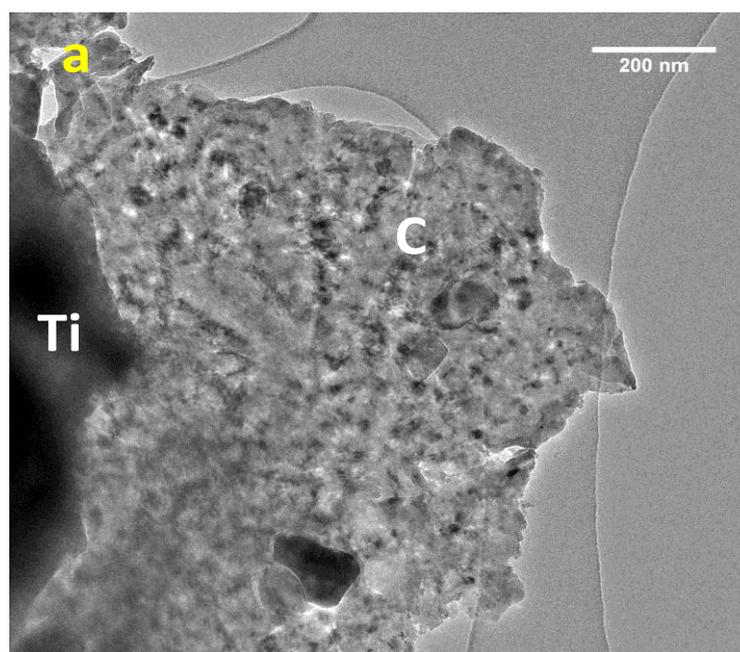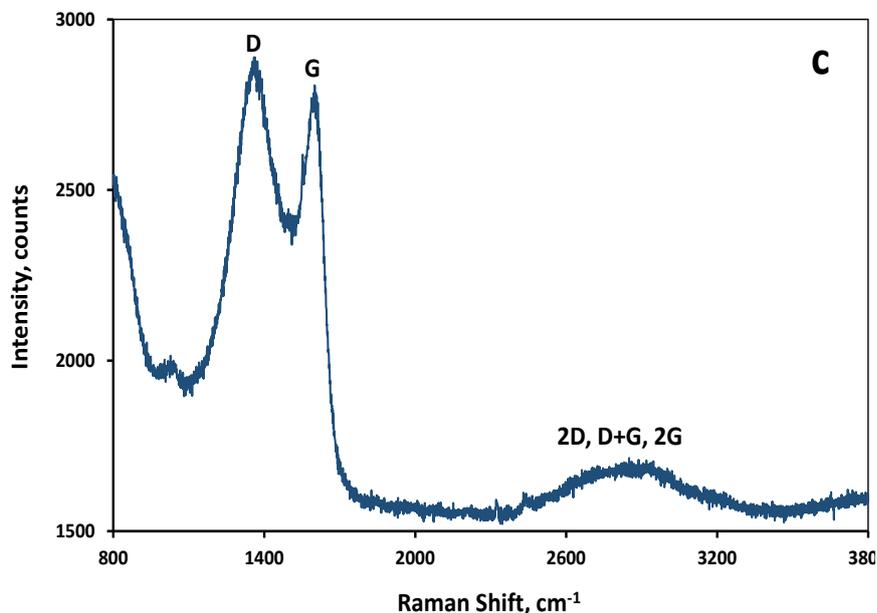
**Figure 2.** HRTEM image (**a**), FTIR (**b**) and Raman (**c**) spectra of a black solid residue formed during the sonolysis of 10%$H_2O$/90%$D_2O$ mixture in the presence of neat CO, $f = 20$ kHz, $P_{ac}$ = 19±1 W, T = 20±1 °C.

Hydrogen released during water sonolysis is enriched with light isotope. Figure 3a reveals several striking dependencies of H/D isotope separation factor, $\alpha_H$, as a function of the carrier gas and $H_2O$/$D_2O$ ratio. An increase in CO content in the saturating gas results in a drastic enhancement of the H/D KIE reaching a maximum $\alpha_H$ value of 14.6±1.8 for pure CO. For comparison, the highest $\alpha_H$ value reported for pure Ar is about 2.15±0.20.[14] These effects are much larger than H/D KIE of water molecule thermal dissociation determined by zero-point energy difference of the ground states for OH/OD bonds ($\Delta E$ = 5.89 kJ mol$^{-1}$) and estimated as $\alpha_H = exp(\Delta E/RT_g) = 1.15$ at $T_g$ = 5000 K. In terms of plasma chemical approach, such a strong sensitization of H/D KIE can be attributed to the essential difference in the reaction pathways with Ar and CO.

In Ar, sonochemical splitting of $H_2O$ would occur by ionization via electron impact or by dissociative excitation transfer between metastable argon Ar* and water molecule:

$$Ar \text{ —)))} \rightarrow Ar^+ + e^- \ (15.76 \text{ eV}) \tag{10}$$

$$e^- + Ar \rightarrow Ar^* + e^- \ (11.72 \text{ eV}) \tag{11}$$

$$e^- + H_2O \rightarrow 2e^- + H_2O^+ \ (12.65 \text{ eV}) \tag{12}$$

$$Ar^* + H_2O \rightarrow Ar + H + OH^{\bullet} \ (5.1 \text{ eV}) \tag{13}$$

In low electron density plasmas, collisions between Ar* and $H_2O$ are responsible for more than 60% of H and $OH^{\bullet}$ production.[25] Generally speaking, process **13** is equivalent to the thermal homolytic dissociation of $H_2O$ and therefore should not exhibit a significant H/D KIE. In addition, electron attachment to $OH^{\bullet}$ radical[26] would decrease the electron density inside the bubble leading to the diminishing of ionization reaction pathway. It is important to emphasize that water splitting via dissociative ionization would exhibit large H/D KIE as it will be discussed further below.

The lower ionization potential of CO compared to Ar provides more efficient ionization of $H_2O$ (reaction **12**) and vibrational excitation of CO as well:

$$CO \longrightarrow))) \rightarrow CO^+ + e^- \ (14.01 \ eV) \tag{14}$$

$$e^- + CO \rightarrow CO^* + e^- \ (5.5 \ eV) \tag{15}$$

In addition, scavenging of $OH^{\bullet}$ radicals with CO would minimize electron loss in the sonochemical plasma via electron attachment to $OH^{\bullet}$ radical. It is therefore conceivable that the dissociative ionization of $H_2O$ plays a much more important role in the presence of CO than in Ar. For the understanding of the H/D KIE in the studied systems it is essential that the electron readily forms cluster anions with water, $(H_2O)_n^-$, where the number of water molecules, $n$, varies from ca. 15 to 35 depending on the experimental conditions.[27,28] It should be noted that the electron solvation time is about 0.3-1.0 ps,[25] which is much shorter than the lifetime of the sonochemical plasma (40-350 ps) measured for a single cavitation bubble.[29] In addition, the high intrabubble pressure would favor the formation of electron-water clusters. Therefore, the H/D KIE in the studied system is determined by electron transfer to hydronium species with different isotope compositions through the shell formed by water molecules ($\alpha_H = k_H/k_D$). Considering for simplicity that $[D_2O] > [H_2O]$, the plasma chemical mechanism of hydrogen emission leading to large KIE can be described as follows:

$$e^- + nD_2O \rightarrow (D_2O)_n^- \tag{16}$$

$$D_2O^+ + D_2O \rightarrow OD^{\bullet} + D_3O^+ \tag{17}$$

$$D_3O^+ + HDO \leftrightharpoons D_2O + HD_2O^+ \quad (K > 1) \tag{18}$$

$$(D_2O)_n^- + HD_2O^+ \rightarrow H + (n+1)D_2O \ (k_H) \tag{19}$$

$$(D_2O)_n^- + D_3O^+ \rightarrow D + (n+1)D_2O \ (k_D) \tag{20}$$

It should be noted that the cations $D_3O^+$ and $HD_2O^+$ are formed almost immediately from $D_2O^+$ species upon hydrogen transfer.[30]

In general, the plasma chemical mechanism of sonochemical water splitting is somewhat similar to the mechanisms reported for water radiolysis or electrolysis.[30,31] The latter two processes exhibit anomalous H/D KIE. In electrolysis, $\alpha_H$ values range from 3.8 to 13.3.[30] In radiolysis, very high $\alpha_H$ values of about $10 - 10^2$ observed in frozen solutions have been attributed to quantum electron tunneling.[31] The high H/D KIE reported in this work in the presence of CO strongly supports the idea about electron tunneling in sonochemical processes as well. According to Wentzel-Kramer-Brillouin (WKB) approximation (**21** and Supporting Information),[32] KIE via quantum tunneling is due to the ratio of electron tunneling probabilities, $P_t$, from electron-water cluster toward $HD_2O^+$ and $D_3O^+$ hydronium species.

$$P_t = exp\left\{\frac{-4\pi L}{h}[2m(E_a - E)]^{1/2}\right\}$$
(21)

The $P_t$ is exponentially inversely proportional to the potential barrier width, $L$, and to the square root of the difference between the activation energy, $E_a$, and the kinetic energy of the electron, $E$. In the studied system, the potential barrier width is determined by the electron transfer through several water molecules. It is known that deuteration results in a global change of hydrogen-bonded supramolecular structures.[33,34] Therefore, even a small difference in $HD_2O^+$ and $D_3O^+$ configuration leads to a large H/D KIE. Figure 3a shows that the H/D selectivity increased with increasing $D_2O$ concentration for both saturating gases, Ar/CO and CO. A similar trend reported for water radiolysis has been attributed to the greater lifetime of solvated electron in $D_2O$ compared to $H_2O$,[29] which is consistent with the heterolytic reaction mechanism proposed in this work for sonochemical water splitting.

It should be mentioned that the CO + OH$^{\bullet}$ reaction is also accompanied by an H/D KIE.[35-37] The $\alpha_H$ values depend on pressure and at near room temperature decrease from about 2 at 0.27 bar to about 1.2 at 0.93 bar. Consequently, this effect would be insignificant in sonochemical process because of the high pressure developed within collapsing bubbles. Numerical simulation of single bubble cavitation suggested that two other processes (**22, 23**) could contribute to the sonochemical hydrogen production during water sonolysis.[40,41] However, both reactions involve homolytic splitting of OH bonds and according to the zero-point energy approximation mentioned above should not exhibit significant H/D KIE at $T_g = 5000$ K.

$$H + OH^{\bullet} \rightarrow H_2 + O$$
(22)

$$H + H_2O \rightarrow H_2 + OH^{\bullet}$$
(23)

In contrast to hydrogen, the simultaneously released $CO_2$ is enriched with heavier isotope $^{13}C$ during the studied process. Figure 3b shows that the $\alpha_C$ value equals $1.26\pm0.05$ whatever the used carried gas or water isotopic composition. As mentioned above, the inverse $^{13}C/^{12}C$ KIE is most likely to be attributed to CO disproportionation via *V-V* pumping mechanism (reaction **6**). In general, for a strongly non-equilibrium process ($T_v > T_g$), the value of isotope separation factor can be expressed as[7]

$$\alpha \approx exp\left[\frac{\Delta\omega}{\omega}E_a\left(\frac{1}{T_g} - \frac{1}{T_v}\right)\right]$$
(24)

where $\frac{\Delta\omega}{\omega}$ is the relative isotopic shift of oscillation frequency and $E_a$ is the activation energy. In non-equilibrium plasmas, heavy isotopes react faster due to higher vibrational temperature. It is interesting to note that the $^{13}C/^{12}C$ isotopic selectivity in sonochemistry seems to be lower than in non-equilibrium plasmas generated by electric discharge in CO gas where the $\alpha_C$ value can reach 2 or 3 at near room $T_g$ temperature (38, 39). This difference can be attributed to the high gas temperature inside the bubble leading to a drop of $\alpha_C$ value according to equation **24**. Using the values of $\frac{\Delta\omega}{\omega} = 0.041$ , $E_a = 6$ eV, $T_g = 0.43$ eV, and $T_v = 5.5$ eV available in the literature for CO molecule,[7] the estimated $\alpha_C$ value to be equal to 1.7, that is still larger than

the experimental value. The main reason of such discrepancy would be that the $^{13}C$-enriched $CO_2$ originated from CO disproportionation is diluted by a much less enriched $CO_2$ formed by CO oxidation with $OH^\bullet$ radical.
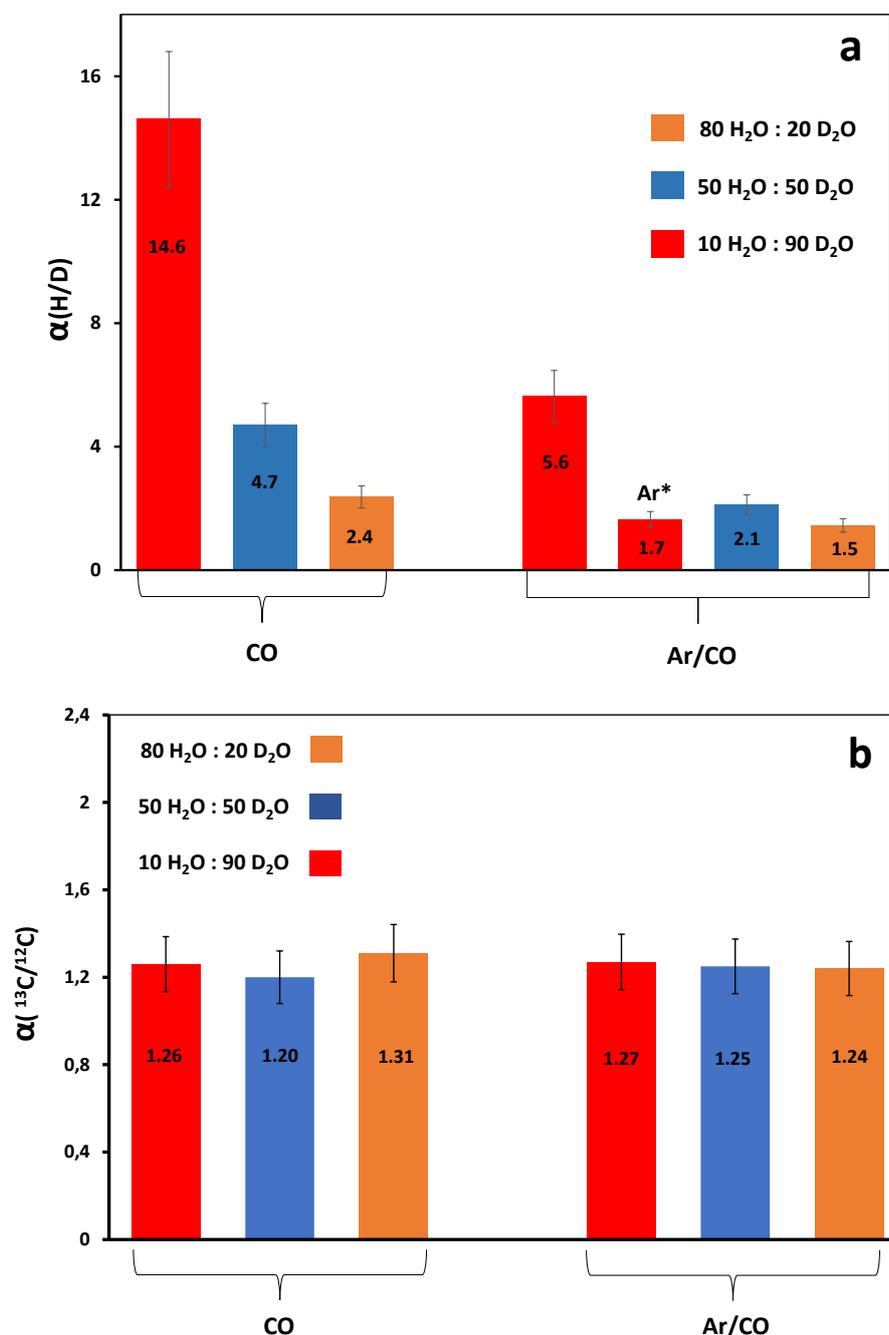


**Figure 3. (a)** H/D isotope separation factor for released hydrogen as a function of the carrier gas and $H_2O/D_2O$ ratio. Ar* is the value of H/D $\alpha_H$ reported for 10vol.% $H_2O/D_2O$ mixture in pure Ar,[14] ($f$ = 20 kHz, $P_{ac}$ = 19±1 W). **(b)** $^{13}C/^{12}C$ isotope separation factor for released $CO_2$ as a function of the carrier gas and $H_2O/D_2O$ ratio. Measured initial $(^{13}C/^{12}C)_0$ ratio equal to $(1.12\pm0.05)\cdot10^{-2}$ is close to the natural abundance of $^{13}C$ isotope.

In summary, this study provides new insights into the origin of sonochemical activity. Large H/D KIE values boosted by CO were observed during the ultrasonic treatment of $H_2O/D_2O$ mixtures and indicate an electron quantum tunneling mechanism. The surprisingly high sonochemical activity of CO in water leading to the emission of $CO_2$ and formation of solid carbonaceous products, as well as an anomalous inverse $^{13}C/^{12}C$ KIE revealed in this work are made possible by the formation of a non-equilibrium plasma inside the cavitation bubbles. The major finding of this work is that quantum effects are indeed important to understand the chemical processes triggered by acoustic cavitation. In this view, sonochemistry may be considered in light of the Third Reactivity Paradigm. This term was recently introduced by Schreiner to highlight the importance of quantum effects for the control of chemical reactions along with thermodynamics and kinetics as factors that can determine the reaction pathway.[42] Quantum effects in sonochemistry open new perspectives in terms of selectivity and efficiency of the chemical processes driven by cavitation and bridge the gap between sonoluminescence and kinetics of many sonochemical reactions, which is still not understood in terms of quasi-adiabatic heating approach.

EXPERIMENTAL METHODS

The experiments were performed using 20 kHz ultrasound. The thermostated sonochemical reactor sparged with saturating gas has been described in our previous studies[12,14] and is shown in Figure S1. The temperature in the reactor during the process was maintained at a steady-state temperature of 20±1°C. The specific absorbed acoustic power, $P_{ac}$ = 19±1 W, transmitted to the solution was measured by conventional thermal probe method. Formation of $H_2$, HD, $D_2$, $^{13}CO_2$, and $^{12}CO_2$ isotopic species was monitored in the outlet gas by mass spectrometry. Hydrogen peroxide in sonicated solutions was measured by absorption spectroscopy with the formation of a colored Ti(IV) peroxide complex ($\lambda$ = 410 nm, $\varepsilon$ = 726 $cm^{-1}$ $M^{-1}$). Further experimental details are described in Supporting Information.

ASSOCIATED CONTENT

**Supporting Information**

The Supporting Information is available free of charge at

Description of the sonochemical reactor, procedures of H/D and $^{13}C/^{12}C$ isotopic analysis, details of $H_2O_2$, TOC, HRTEM, FTIR, Raman, and ion-chromatography analysis, WKB equation.

AUTHOR INFORMATION

**Corresponding Author**

**Sergey I. Nikitenko** - *ICSM, Univ Montpellier, UMR 5257, CEA, CNRS, ENSCM, Marcoule, France*; orcid.org/ 0000-0003-4802-6325;

Email: serguei.nikitenko@cea.fr

**Authors**

**Tony Chave -** *ICSM, Univ Montpellier, UMR 5257, CEA, CNRS, ENSCM, Marcoule, France*

**Matthieu Virot** *- ICSM, Univ Montpellier, UMR 5257, CEA, CNRS, ENSCM, Marcoule, France*

**Rachel Pflieger -** *ICSM, Univ Montpellier, UMR 5257, CEA, CNRS, ENSCM, Marcoule, France*

**Notes**

There are no conflicts to declare.

REFERENCES

(1) Richards, W. T.; Loomis, L. A. The Chemical Effects of High Frequency Sound Waves. I. A Preliminary Survey. *J. Amer. Chem. Soc*. **1927**, 49, 3086-3100.

(2) Schmitt, F. O.; Johnson, C. H.; Olson, A. R. Oxidation Promoted by Ultrasonic Radiation. *J. Amer. Chem. Soc*. **1929**, 51, 370-375.

(3) Suslick, K. S.; McNamara, W. B.; Didenko, Y. Hot Spot Conditions During Multi-Bubble Cavitation, In: *Sonochemistry and Sonoluminescence, NATO ASI Series C: Mathematical and Physical Sciences*, Crum, L. A.; Mason, T. J.; Reisse, J. L.; Suslick, K; S. Eds., **1999**, Springer, Dordrecht, Germany.

(4) Pflieger, R.; Brau, H. P.; Nikitenko, S. I. Sonoluminescence from $OH(C^2\Sigma^+)$ and $OH(A^2\Sigma^+)$ Radicals in Water: Evidence for Plasma Formation during Multibubble Cavitation. *Chem. Eur. J*. **2010**, 16, 11801-11803.

(5) Ndiaye, A. A.; Pflieger, R.; Siboulet, B.; Molina, J.; Dufreche, J. F.; Nikitenko, S. I. Nonequilibrium Vibrational Excitation of OH Radicals Generated during Multibubble Cavitation in Water. *J. Phys. Chem. A*, **2012**, 116, 4860-4867.

(6) Pflieger, R.; Ouerhani, T.; Belmonte, T.; Nikitenko, S. I. Use of $NH(A^3\Pi-X^3\Sigma^-)$ Sonoluminescence for Diagnostics of Nonequilibrium Plasma Produced by Multibubble Cavitation. *Phys. Chem. Chem. Phys*. **2017**, 19, 26272-26279.

(7) Fridman, A. *Plasma Chemistry*. **2008**, Cambridge University Press, Cambridge, USA.

(8) Flannigan, D. J.; Suslick, K. S. Plasma Formation and Temperature Measurement during Single-Bubble Cavitation. *Nature,* **2005**, 434, 52-55.

(9) Flannigan, D. J.; Suslick, K. S. Plasma Line Emission during Single-Bubble Cavitation. *Phys. Rev. Lett*. **2005**, 95, 044301.

(10) Sharipov, G. L.; B. M. Gareev, B. M.; Abdrakhmanov, A. M. Confirmation of Hydrated Electrons Formation during the Moving Single-Bubble Sonolysis: Activation of $Tb^{3+}$ Ion Sonoluminescence by $e^-_{aq}$ Acceptors in an Aqueous Solution. *J. Photochem. Photobiol. A: Chemistry*, **2020**, 402, 112800.

(11) Sharipov, G. L.; Gareev, B. M.; Vasilyuk, K. S.; Galimov, D. I. New Sonochemiluminescence Involving Solvated Electron in Ce(III)/Ce(IV) Solutions. *Ultrason. Sonochem.* **2021**, 70, 105313.

(12) Nikitenko, S. I.; Martinez, P.; Chave, T.; Billy, I. Sonochemical Disproportionation of Carbon Monoxide in Water: Evidence for Treanor Effect during Multibubble Cavitation. *Angew. Chem. Int. Ed.* **2009**, 48, 9529-9532.

(13) Van Hook, W. A. Isotope Effects in Chemistry. *Nukleonika,* **2011***,* 56, 217-240.

(14) Nikitenko, S. I.; Di Pasquale, T.; Chave, T.; Pflieger, R. Hypothesis about Electron Quantum Tunneling during Sonochemical Splitting of Water Molecule. *Ultrason. Sonochem.* **2020**, 60, 104789.

(15) *Engineering Toolbox,* **2003**. Available at: https://www.engineeringtoolbox.com.

(16) Briner, E.; Hoefer, H. Recherches sur L'action Chimique des Décharges Electriques. XIX. Production de L'acide Cyanhydrique et de L'ammoniac par L'arc Electrique en Haute et Basse Fréquences Jaillissant dans les Mélanges Azote Oxyde de Carbone-Hydrogène à la Pression Ordinaire et en Dépression, *Helv. Chim. Acta*, **1940**, 23, 800.

(17) Schlapbach, L.; Zuttel, A. Hydrogen-Storage Materials for Mobile Applications, *Nature,* **2001***,* 414, 353–358.

(18) Jolly, G. S.; McKenney, D. J.; Singleton, D. L.; Paraskevopoulos, G.; Bossard, A. R. Rates of Hydroxyl Radical Reactions. Part 14. Rate Constant and Mechanism for the Reaction of Hydroxyl Radical with Formic Acid, *J. Phys. Chem.* **1986**, 90, 6557-6562.

(19) Anglada, J. M. Complex Mechanism of the Gas Phase Reaction Between Formic Acid and Hydroxyl Radical. Proton Coupled Electron Transfer Versus Radical Hydrogen Abstraction Mechanisms. *J. Am. Chem. Soc*. **2004**, 126, 9809-9820.

(20) Snow, A. W.; Haubenstock, H.; Yang, N.-L. Poly(carbon suboxide). Characterization, Polymerization, and Radical Structure. *Macromolecules*, **1978**, 11, 77-86.

(21) Schmedt auf der Günne, J.; Beck, J.; Hoffbauer, W.; Krieger-Beck, P. The Structure of Poly(carbonsuboxide) on the Atomic Scale: A Solid-State NMR Study. *Chem. Eur. J*. **2005**, 11, 4429-4440.

(22) McGreery, R. L. Advanced Carbon Electrode Materials for Molecular Electrochemistry. *Chem. Rev*. **2008**, 108, 2646-2687.

(23) Evans, W. J.; Lipp, M. J.; Yoo, C.-S.; Cynn, H.; Herberg, J. L.; Maxwell, R. S. High-Pressure Diamond Anvil Cell Studies of Carbon Monoxide – Viscosity, Photochemical Polymerization and Laser Heating. *Chem. Mater.* **2006**, 18, 2520-2531.

(24) Lopez-Salas, N.; Kossmann, J.; Antonietti, M. Rediscovering Forgotten Members of the Graphene Family. *Acc. Mater. Res*. **2020**, 1, 117-122.

(25) Luo, Y.; Lietz, A. M.; Yatom, S.; Kushner, M. J.; Bruggeman, P. J. Plasma Kinetics in a Nanosecond Pulsed Filamentary Discharge Sustained in Ar-$H_2O$ and $H_2O$. *J. Phys. D: Appl. Phys*. **2019**, 52, 044003.

(26) Adriaanse, C.; Sulpizi, M.; Vande Vondele, J.; Sprik, M. The Electron Attachment Energy of the Aqueous Hydroxyl Radical Predicted from the Detachment Energy of the Aqueous Hydroxide Anion. *J. Am. Chem. Soc*. **2009**, 131, 6046-6047.

(27) Paik, D. H.; Lee, I.-R.; I.-R.; Yang, D.-S.; Baskin, J. S.; Zewall, A. H. Electrons in Finite-Sized Water Cavities: Hydration dynamics observed in real time. *Science* **2004**, 306, 672-675.

(28) Svoboda, V.; Michiels, R.; LaForge, A. C.; Med, J.; Stienkemeier, F.; Slaviček, P.; Wörner, H.J. Real-Time Observation of Water Radiolysis and Hydrated Electron Formation Induced by Extreme-Ultraviolet Pulses. *Sci. Adv*. **2020**, 6, eaaz0385.

(29) Hiller, R. A.; Putterman, S. J.; Weninger, K. R. Time-Resolved Spectra of Sonoluminescence. *Phys. Rev. Lett*. **1998**, 80, 1090-1093.

(30) Muto, H.; Matsuura, K.; Nunome, K. Large Isotope Effect due to Quantum Tunneling in the Conversion Reaction of Electrons to H and D Atoms in Irradiated $H_2O$/$D_2O$ Ice. *J. Phys. Chem*. **1992**, 96, 5211-5213.

(31) Bockris, J. O. M.; S. U. Khan, S. U. *Quantum Electrochemistry*, **2012**, Plenum Press, New York, USA.

(32) Meisner, J.; Kästner, J. Atom Tunneling in Chemistry. *Angew. Chem. Int. Ed*. **2016**, 55, 5400-5413.

(33) Benedict, H.; Limbach, H.-H.; Wehlan, M.; Fehlhammer, W.-P.; Golubev, N. S.; Janoschek, R. Solid State ^{15}N NMR and Theoretical Studies of Primary and Secondary Geometric H/D Isotope Effects on Low-Barrier NHN−Hydrogen Bonds. *J. Am. Chem. Soc*. **1998**, 120, 2939–2950.

(34) Shi, C.; Zhang, X.; Yu, C.-H.; Yao, Y.-F.; Zhang, W. Geometric Isotope Effect of Deuteration in a Hydrogen-Bonded Host–Guest Crystal. *Nature Comm*. **2018**, 9, 481.

(35) Feilberg, K. L.; Sellevåg, S. R.; Nielsen, C. J.; Griffith, D. W. T.; Johnson, M. S. $CO + OH \rightarrow CO_2 + H$: the relative reaction rate of five CO isotopologues. *Phys. Chem. Chem. Phys*. **2002**, 4, 4687- 4693.

(36) Chen, W.-C.; Marcus, R. A. On the Theory of the CO+OH Reaction, Including H and C Kinetic Isotope Effects. *J. Chem. Phys*. **2005**, 123, 094307.

(37) Feilberg, K. L.; Johnson, M. S.; Nielsen, C. J. Relative Rates of Reaction of [13]C[16]O, [12]C[18]O, [12]C[17]O and [13]C[18]O with OH and OD Radicals. *Phys. Chem. Chem. Phys*. **2005**, 7, 2318-2323.

(38) Bergman, R. C.; Homicz, G. F.; Rich, J. W.; Wolk, G. L. [13]C and [18]O Isotope Enrichment by Vibrational Energy Exchange Pumping of CO. *J. Chem. Phys*. **1983**, 78, 1281-1292.

(39) Mori, S.; Akatsuka, H.; Suzuki, M. Carbon and Oxygen Isotope Separation by Plasma Chemical Reactions in Carbon Monoxide Glow Discharge. *J. Nucl. Sci. Technol*. **2001**, 38, 850-858.

(40) Yasui, K.; Tuziuti, T.; Kozuka, T. ; Towata, A.; Iida, Y. Relationship Between the Bubble Temperature and Main Oxidant Created Inside an Air Bubble Under Ultrasound. *J. Chem. Phys*. **2007**, 127, 154502.

(41) Yasui, K.; Tuziuti, T.; Sivakumar, M. ; Iida, Y. Theoretical Study of Single-Bubble Sonochemistry. *J. Chem. Phys*. **2005**, 122, 224706.

(42) Schreiner, P. R. Tunneling Control of Chemical Reactions: The Third Reactivity Paradigm. *J. Am. Chem. Soc*. **2017**, 139, 15276-15283.